

IAC-14,B2,8-YPVF.3,7,x21781

Cross-band aided acquisition on HEO orbit

**Mr. Jia Tian**

CAST-Xi'an Institute of Space Radio Technology, China, [jia1093291643.tian@gmail.com](mailto:jia1093291643.tian@gmail.com)

**Mr. Yanguang Wang**

CAST-Xi'an Institute of Space Radio Technology, China, [wggaily@163.com](mailto:wggaily@163.com)

**Prof. Wei Wang**

CAST-Xi'an Institute of Space Radio Technology, China, [wwei98@163.com](mailto:wwei98@163.com)

**Prof. Pingyan Shi**

CAST-Xi'an Institute of Space Radio Technology, China, [Shipingyan@gmail.com](mailto:Shipingyan@gmail.com)

**Mr. Vincenzo Capuano**

École Polytechnique Fédérale de Lausanne (ESPLAB), Switzerland, [vincenzo.capuano@epfl.ch](mailto:vincenzo.capuano@epfl.ch)

**Dr. Jérôme Leclère**

École Polytechnique Fédérale de Lausanne (ESPLAB), Switzerland, [jerome.leclere@epfl.ch](mailto:jerome.leclere@epfl.ch)

**Dr. Cyril Botteron**

École Polytechnique Fédérale de Lausanne (ESPLAB), Switzerland, [cyril.botteron@epfl.ch](mailto:cyril.botteron@epfl.ch)

**Prof. Pierre-André Farine**

École Polytechnique Fédérale de Lausanne (ESPLAB), Switzerland, [pierre-andre.farine@epfl.ch](mailto:pierre-andre.farine@epfl.ch)

Global positioning system (GPS) has been demonstrated to be a valid and efficient system for various space applications in low Earth orbit (LEO) and medium Earth orbit (MEO), such as for location determination and time synchronization. However, in highly elliptical and high Earth orbits (HEO), the number of existing space applications is much smaller because of the very weak power of the received signals and the bad geometric dilution of precision (GDOP). To counteract these problems, one method is to add an L5 processing module to the existing L1 C/A receiver module. Indeed, tracking the L5 signal brings several benefits: 1) a higher ranging precision; 2) a pilot channel allowing long integration times, which is helpful for both acquisition and tracking. But this also implies several drawbacks, especially in resource restricted conditions: 1) the length of the fast Fourier transforms (FFTs) and the amount of memory needed for the L5 acquisition module is huge; 2) the acquisition time is very long because of the secondary code and large frequency search space due to the long integration time. In this paper, a cross-band aided acquisition method for the L1&L5 signals is presented, which satisfy the requirements for extremely high sensitive environment without any further assistance. Compared to a traditional architecture that would acquire the L1 and L5 signals sequentially, this method acquires the L1 signal in the first place because its structure is simpler and there is no need to search the secondary code, then uses this information to reduce the code and frequency search space of the L5 signals. This brings huge benefits to the receiver: 1) the resources needed for the L5 acquisition are tremendously reduced; 2) the acquisition time for the L5 signal is considerably reduced. The implementation on an Altera Stratix III FPGA shows that about 7 % of the logic, 18 % of the multipliers and 47 % of the memory can be saved with the proposed method, while the acquisition time is reduced by 99 %.

## I. INTRODUCTION

Although GPS was designed for terrestrial users, nowadays, it has been demonstrated as an effective and efficient system for a considerable number of space applications. In [1], there is a projection that based on the GPS constellation, over the next twenty years approximately 60 % of space missions will operate in LEO (which ranges from an altitude of 160 km to about

2000 km), 35 % of space missions will operate at higher altitudes up to geostationary Earth orbit (GEO, altitude of approximately 35,786 km), and the reminding 5% will be a Cislunar / Interplanetary or HEO missions.

The main reasons why there are less space applications on HEO orbit are because the received GNSS signals are very weak, which makes their acquisition and tracking difficult; and the GDOP

becomes very large. It is well known (see, e.g., [2]) that the position error can be expressed as the product between a geometric factor (the composite effect of the relative satellite-user geometry on the GPS solution error) and a pseudorange error factor (a statistical sum of the contributions from each of the ranging error sources). Without considering additional constellations providing additional satellites, we cannot easily reduce the GDOP in HEO orbits but we can try to reduce the pseudorange error. Several solutions have been proposed, as in [3]. One method is to use the L5 signal in addition to the L1 C/A. Indeed, the chipping rate of the L5 signal is 10 times higher than that of L1 (10.23 Mchip/s instead of 1.023 Mchip/s), which means that the pseudorange error will be 10 times smaller than that of L1. However, not all the GPS satellites transmit the L5 signal currently, which means that the receiver should have the capability to process L1 and L5 signals at the same time. Moreover, the resources needed for the L5 acquisition are huge because of the higher sampling rate and the presence of a secondary code on the pilot channel.

Within this context, this paper aims to develop an acquisition method that can perform the L1 and L5 signals acquisition at the same time with less resources and time. Section II presents the orbit analysis and link budget, while Section III reports some parameters chosen in this paper. In particular, the individual acquisition of the L1 signal and the L5 signal are discussed in Section IV and V, respectively, while the acquisition of L5 signal aided by the L1 acquisition is presented in Section VI.

## II. THE ORBIT ANALYSIS AND LINK BUDGET

The Earth - Moon transfer orbit (MTO) is one example of highly elliptical orbit in which a spacecraft travels from LEO to HEO. The analysis below will focus on a generic MTO.

The lunar transfer trajectory is depicted in Fig. 1, and the parameters of the orbit are reported in Table 1.

The antenna gain pattern for GPS Block II/IIA/IIR satellites can be found in [4]. For our evaluation, two degrees have been considered,  $10^\circ$ , corresponding to the maximum power (maximum of the main lobe) equal to 16 dBi, and  $32^\circ$ , corresponding to the maximum value of the first side lobe equal to 2 dBi. The GPS satellites transmit power is 27 W, i.e. about 14.3 dBW [5]. Thus, the equivalent isotropically radiated power (EIRP) for these two angles is:  $EIRP(10^\circ) = 30.3$  dBW and  $EIRP(32^\circ) = 16.3$  dBW.

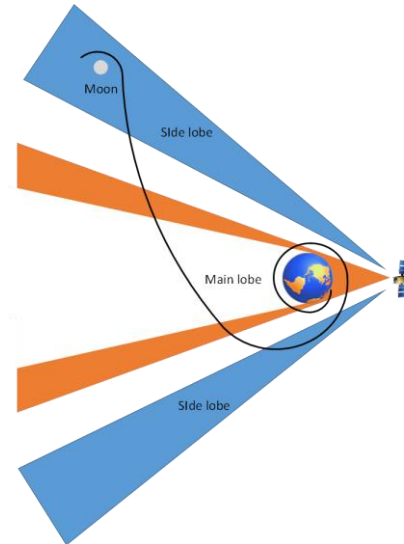


Fig. 1: A lunar transfer trajectory from the Earth.

Parameters	Values
Height of the orbit around the Moon [16] (km)	100
Earth radius (km)	6378
Lunar radius (km)	1738
Highest distance between the Earth and the Moon (km)	405 696
GPS semi-major axis (km)	26 560

Table 1: Parameters of the lunar transfer trajectory.

According to Table 1, the theoretical longest distance between a GPS satellite and a spacecraft orbiting around the Moon is

$$d_{lunar} = 26560 + 405696 + 1738 + 100 = 434094 \text{ km.} \quad (1)$$

Although this value is slightly longer than the real maximum line of sight distance between the receiver and a GNSS satellite, we use it to be conservative.

The corresponding free space loss is thus

$$L_{free} = 20 \log_{10} \left( \frac{\lambda_{L1}}{4\pi d_{lunar}} \right) = -209.1 \text{ dB,} \quad (2)$$

where  $\lambda_{L1}$  is the wavelength of the L1 signal ( $\lambda = c / f_{L1} \approx 19$  cm with  $c$  the speed of light and  $f_{L1} = 1575.42$  MHz).

The maximum received power from the main lobe and the first side lobe is given by Eq. (3) and (4), respectively.

$$P_R(10^\circ) = EIRP(10^\circ) + L_{free} + L_{pol} + L_{atm} + G_r = -139.7 \text{ dBm,} \quad (3)$$

$$P_R(32^\circ) = EIRP(32^\circ) + L_{free} + L_{pol} + G_r = -153.2 \text{ dBm,} \quad (4)$$

where  $L_{pd}$  is the polarization loss, equal to  $-0.4$  dB [2],  $L_{am}$  is the atmosphere loss, equal to  $-0.5$  dB [2], and  $G_r$  is the antenna gain of the receiver, taken as 10 dBi.

The noise figure of the whole front-end including cable, interface and LNA is as assumed to be 2 dB, so the IF noise power density [5] is

$$N_0 = -174 \text{ dBm/Hz} \quad (5)$$

Thus, the carrier-to-noise ratio is

$$C/N_0(10^\circ) = P_R(10^\circ) - N_0 = 34.3 \text{ dBHz} \quad (6)$$

$$C/N_0(32^\circ) = P_R(32^\circ) - N_0 = 20.8 \text{ dBHz}.$$

In order to leave some margin for hardware implementation, for the following, our targeted  $C/N_0$  for GPS L1 C/A is 16 dBHz.

### III. SYSTEM SETUP

#### III.I Source Generator

The GPS signals are generated by a Spirent GSS8000 simulator, which includes facilities to accommodate the special needs of a space-based receiver testing, including [6]:

- Full account for the double atmosphere effect of signals passing through the atmosphere twice for the GPS satellites located on the far side of the Earth.
- Realistic satellite transmit-antenna patterns.
- Spacecraft models and spacecraft motion models.
- Ability to define trajectory data in real time.

The simulation results in [7] show that the carrier frequency can be affected by a Doppler up to 35 kHz.

#### III. II Front-end Characteristics

The front-end we use is the Fraunhofer Triband front-end [8]. Its main parameters are given in Table 2.

Since the sampling frequency is relatively high, a downsampling (down convert, low-pass filter and decimation) is performed before the acquisition process. After the downsampling, the sampling frequency is 4.096 MHz for the L1 signal, and 20.48 MHz for the L5 signal. The samples after the down sampling are saved in DDR2-SDRAM on our FPGA DE3 platform [9].

#### III. III FPGA Board characteristic

The FPGA board used is the Terasic DE3 System, which embeds an Altera Stratix III FPGA (EP3SE260F1152). The resources available in this FPGA are:

- 135 200 adaptive logic modules (ALMs), equivalent to 254 400 logic elements (LEs),
- 864 blocks of 9216 bits (M9K),
- 48 blocks of 147 456 bits (M144K = 16 M9K),
- 768 18-bit multipliers (DSP).

Signal	Parameters	Values
GPS L1	Analog IF (MHz)	53.78
	Digital IF (MHz)	12.82
	Sampling rate (MHz)	40.96
	Resolution (bits)	2
	Output format	real
GPS L5	Analog IF (MHz)	53.7
	Digital IF (MHz)	12.74
	Sampling rate (MHz)	40.96
	Resolution (bits)	4
	Output format	real

Table 2: Parameters of Fraunhofer Triband front end [8]

## IV. ACQUISITION OF THE L1 SIGNAL

### IV. I Theoretical Analysis

The full bit method proposed in [10] to handle the GPS L1 C/A data bit transitions has been selected in this paper, with 4 branches, as this implementation will achieve a good balance between the coherent integration gain and the FPGA resources. Therefore, the corresponding coherent integration time is 20 ms and the step between two Doppler bins tested is 25 Hz. The evaluation of the total integration time is based on Chapter 6 of [5], where it is stated that to make the acquisition successfully, the signal-to-noise ratio (SNR) after the correlation should be higher than 14 dB.

The results of the theoretical analysis are summarized in Table 3.

Parameters	Values
Sampling rate after down-sampling (MHz)	4.096
Coherent integration time (s)	0.02
Ideal coherent gain (dB)	46.1
IF-filtering loss (dB)	0
Quantization loss (dB)	0.55
Frequency mismatch loss (dB)	0.9
Code alignment loss (dB)	1.16
Data bit alignment loss (dB)	1.16
Coherent SNR (dB)	-4.77
Squaring loss (dB)	5.5
Number of non-coherent integrations	268
Final SNR (dB)	14

Table 3 Theoretical analysis of L1 acquisition

In order to make the final SNR higher than 14 dB, the number of non-coherent integration needed is 268, so the whole integration time is 5.36 s.

#### IV. II Architecture and resource analysis

The implementation architecture is shown in Fig. 2. The details of the FFT implemented in FPGA are presented in Table 4.

Parameters	Values
Transform Length (points)	4096
Data Input Precision (bits)	18
Twiddle Precision (bits)	18
I/O Data Flow	Streaming

Table 4: Implementation details of the FFT

The information about the implementation of other modules is shown below:

- The carrier and code generator are based on a NCO.
- The control module will keep each start of coherent integration of the 4 branches delayed by 5 ms.
- The magnitude is computed using the Robertson approximation.
- The coherent and non-coherent accumulator are memory-based.
- The peak extraction module calculates the peak value, peak index, mean value and standard deviation value.
- The determination module calculates the SNR and selects the biggest one.

The required FPGA resources of each module in Fig. 2 are given in Table 5, according to the models described in [11]. The resources needed for the acquisition of the L1 C/A signal represent 13.99 % of the ALMs available in the FPGA, 22 % of the DSP and 21.45 % of the RAM.

#### IV. III Acquisition time analysis

The time spent to search one frequency bin is defined as

$$T_{FB} = \frac{f_{S,L1} T_I}{f_{FPGA}} = \frac{4.096 \cdot 10^6 \times 5.36}{204.8 \cdot 10^6} = 107.2 \text{ ms} \quad (7)$$

where  $f_{S,L1}$  is the sampling rate of L1 after the downsampling,  $T_I$  is the total integration time, and  $f_{FPGA}$  is the processing frequency of the FPGA. Note that the latency due to the FFTs is not considered here, since it represents a very small portion of the total.

Based on the simulation results (see Section III.I), the frequency search space is  $\pm 35$  kHz. Thus, with a frequency step of 25 Hz, there are 2800 frequency bins to search. So the acquisition time is:

$$T_{A,1} = T_I + N_{FB,1} T_{FB} = 5.36 + 2800 \times 107.2 \times 10^{-3} \approx 305.52 \text{ s} \quad (8)$$

### V. ACQUISITION OF THE L5 SIGNAL

#### V. I Theoretical Analysis

Because the information about the antenna gain pattern of L5 is not yet published (to the best knowledge of the authors), we assumed in this paper that the antenna gain pattern of L5 is same as that of L1.

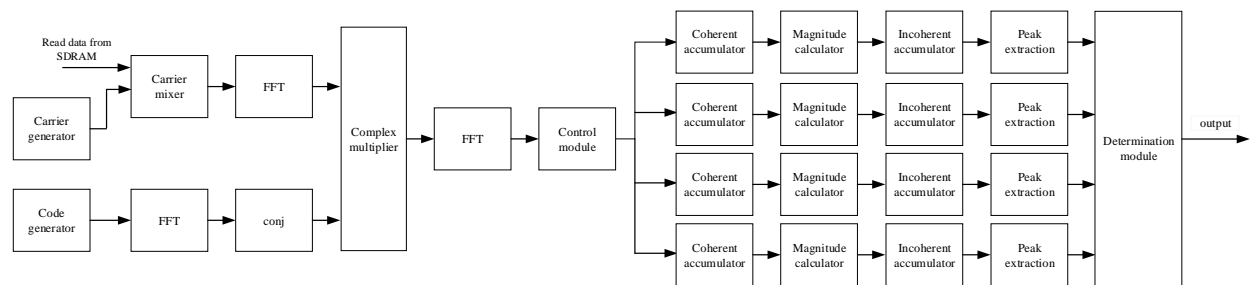


Fig. 2: Implementation architecture of L1C/A acquisition.

Module	ALMs	DSP	FPGA RAM (bit)	DDR2 SDRAM (bit)
RAM for saving the data				$786.5 \times 10^6$
Carrier generator	32			
Carrier mixer	56			

Code generator	37.5		1023	
FFT core	3430	32	127 344	
Complex multiplier		4		
IFFT core	3430	32	127 344	
Magnitude calculator	73			
Coherent accumulator	58		188 416	
Non-coherent accumulator	45		135 168	
Peak extraction	68			
Control module	23			
Determination module	31			
Total	18 916	169	3.226×10 <sup>6</sup>	

Table 5 Resources requires for the L1 acquisition (Fig. 2).

The carrier frequency of the L5 signal is 1176.45 MHz, which means that the free space loss of the L5 signal (-206.6 dB) is smaller than that of the L1 signal (-209.1 dB). Therefore, the targeted  $C/N_0$  for the L5 signal is 18.5 dBHz in this paper. Compared with L1, the frequency search space of L5 is decreased too, and equals  $\pm 26.1$  kHz.

The selected acquisition method of L5 signal is the double block zero padding (DBZP) proposed in [12] to handle the bit transition due to the secondary code, which is much suitable for the acquisition of the L5 pilot channel.

The coherent integration gain analysis is shown in Table 7.

From Table 7, it can be seen that the number of frequency bins increases when the coherent integration time increases. The longer is the coherent integration time, the smaller is the maximum tolerable Doppler rate (the maximum tolerable to avoid a shift between two frequency bins). So in order to achieve the minimum processing time and biggest tolerable Doppler rate, a value of 20 ms coherent integration time is chosen.

## V. II Architecture and resource analysis

The traditional L5 acquisition architecture is shown in Fig. 3 and the FPGA resources needed for this structure are presented in Table 6.

So the whole resources needed are ALMs: 10.81 %, DSP: 17.71 %, RAM: 47.32 %.

## V. III Acquisition time analysis

The time spent to search one frequency bin is defined as

$$T_{FB} = \frac{f_{s,L5} T_I N_{DBZP} N_{sec}}{f_{FPGA}} = \frac{20.48 \times 10^6 \times 1.58 \times 2 \times 20}{204.8 \times 10^6} = 6.32 \text{ s} \quad (9)$$

$C/N_0$ considered (dBHz)	18.5
IF SNR (dB)	- 54.6
Sampling rate after down-sampling (MHz)	20.48

where  $f_{s,L5}$  is the sampling rate of L5 after downsampling,  $N_{DBZP}$  is the factor caused by the DBZP method, and  $N_{sec}$  is the factor caused by the secondary code of L5 pilot channel.

The acquisition time is then

$$T_{A,1} = T_I + N_{FB,1} T_{FB} = 1.58 + 2088 \times 6.32 \approx 13198 \text{ s} \quad (10)$$

Therefore, it can be seen that without the assistance of L1, the resources and the acquisition time are huge, which is fatal for space applications with limited resources.

Module	ALMs	DSP	FPGA RAM (bit)
Carrier mixer	56		
Code generator	39.1		10230
FFT core	4230	40	1450022
IFFT core	5782	52	2629206
Complex multiplier		4	
Magnitude calculator	73		
Coherent accumulator	60		942080
Non-coherent accumulator	47		634880
Peak extraction	68		

Table 6 Resources required for L5 acquisition

Coherent integration time (s)	0.02	0.04	0.08
Ideal coherent gain (dB)	56.1	59.1	62.1
IF filtering loss (dB)	0	0	0
Quantization loss (dB)	0.05	0.05	0.05
Frequency mismatch loss (dB)	0.9	0.9	0.9
Code alignment loss (dB)	2.5	2.5	2.5
Data bit alignment loss (dB)	0	0	0
Coherent SNR (dB)	-1.95	1.06	4.07
Squaring loss (dB)	2.98	0.49	1.48
Number of non-coherent integration	79	23	7
Final SNR (dB)	14	14	14
Total integration time (s)	1.58	0.92	0.56
Number of frequency bins	2088	4176	8352
Maximum tolerable Doppler rate (Hz/s)	15.82	13.59	11.16

Table 7 Coherent integration gain of L5 signal.

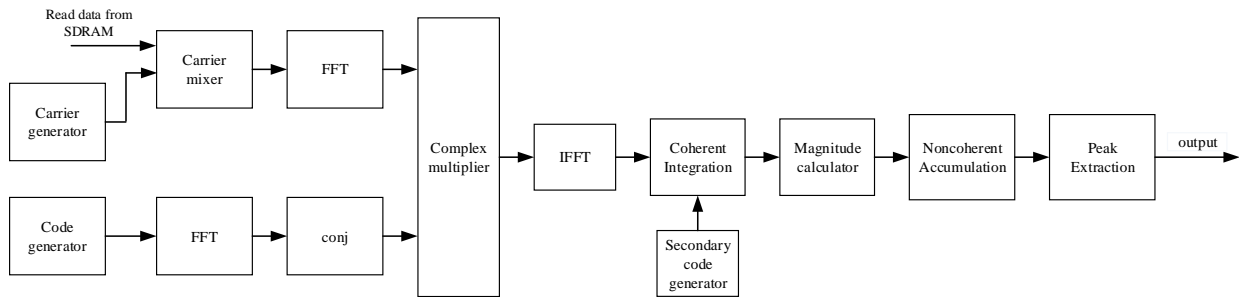


Fig. 3 Traditional L5 acquisition structure.

## VI. ACQUISITION OF THE L5 SIGNAL AIDED BY THE L1 ACQUISITION

### VI. I Theoretical Analysis

When the L1C/A signal is acquired, the code phase and Doppler frequency are precisely known. Since the L1 and L5 signals from a same satellite are synchronized and experience about the same delay, this information can be used to tremendously decrease the frequency search space and code phase search space for the L5 signal.

#### Frequency search space

The frequency shift of the received signal is composed of 2 parts, one is the shift caused by the Doppler effect, and the other is the shift caused by the oscillator frequency shift.

$$f_{\text{offsetL5}} = f_{\text{dopplerL5}} + f_{\text{oscillatorL5}} \quad (11)$$

$$f_{\text{offsetL1}} = f_{\text{dopplerL1}} + f_{\text{oscillatorL1}}$$

where  $f_{\text{offsetL5}}$  is the real frequency shift of L5 signal,

$f_{\text{offsetL1}}$  is the real frequency shift of L1 signal,

$f_{\text{dopplerL5}}$  and  $f_{\text{dopplerL1}}$  are the Doppler shift of L5 and L1 signals,  $f_{\text{oscillatorL5}}$  and  $f_{\text{oscillatorL1}}$  are the oscillator frequency shifts of L5 and L1 signals, respectively.

Because of the frequency difference of L1 and L5, the relationship between  $f_{\text{dopplerL5}}$  and  $f_{\text{dopplerL1}}$  is

$$f_{\text{dopplerL5}} = \frac{1176.45 \text{ MHz}}{1575.42 \text{ MHz}} \times f_{\text{dopplerL1}} = 0.7468 \times f_{\text{dopplerL1}} \quad (12)$$

The oscillator frequency shift is caused by the local oscillator, and the ideal local oscillator frequency is defined as

$$f_{LO} = M_{LO} f_{REF}, \quad (13)$$

where  $M_{LO}$  is a rational number and  $f_{REF}$  is the ideal reference frequency. However, the reference oscillator is not perfect, and consequently its actual frequency is not exactly  $f_{REF}$ . The accuracy of an oscillator is usually defined in ppm. To take into account the accuracy of the reference oscillator, we will denote  $f_{ref}$  the actual reference frequency, which is defined as

$$f_{ref} = f_{REF} \times (1 + \beta), \quad (14)$$

where  $\beta$  represents the oscillator accuracy. For example, if the oscillator accuracy is 1 ppm,  $\beta=10^{-6}$ . Thus, the oscillator frequency shift can be calculated as

$$\begin{aligned} f_{oscillatorL5} &= f_{LO\_L5} \times \beta \\ f_{oscillatorL1} &= f_{LO\_L1} \times \beta \end{aligned} \quad (15)$$

Because the frequency will finally be converted to baseband,  $f_{LO\_L1}=1575.42\text{MHz}$ ,  $f_{LO\_L5}=1176.45\text{MHz}$ .

Therefore, the relationship between  $f_{oscillatorL5}$  and  $f_{oscillatorL1}$  is

$$f_{oscillatorL5}=0.7468 \times f_{oscillatorL1}. \quad (16)$$

Therefore,  $f_{offsetL5}=0.7468 \times f_{offsetL1}$ , which means that there is no need to search the frequency of the L5 signal when the L1 signal is acquired.

#### Group delay analysis

The time reference between the two GPS bands must take into account the presence of misalignments between the two bands due to equipment group delay and transmission delays through the ionosphere. As in general equipment, group delays are in the order of 1 ns, they are considered negligible with respect to ionosphere effects [13].

The maximum ionosphere delay proposed in [14] is 150m. Therefore, using the equations presented in [15], the maximum ionosphere delay for the composite L1-L5 signal is calculated in Eq. (17).

$$\Delta = 150 \times \left( 1 - \left( \frac{1575.42 \text{ MHz}}{1176.45 \text{ MHz}} \right)^2 \right) = 119 \text{ m}. \quad (17)$$

So the code phase search space of L5 caused by ionosphere delay is almost 4 chips.

#### Code phase search space

The chipping rate is 1.023 MHz for the L1 signal and 10.23 MHz for the L5 signal, which means that 1 chip for L1 represents 10 chips for L5. The code phase of L5 can be calculated in Eq. (18).

$$C_{L5} = 10 C_{L1} \quad (18)$$

where  $C_{L1}$  is the code phase of L1 and  $C_{L5}$  is the code phase of L5.

The ambiguity of the L1 code phase is 0.25 chip (4 samples per chip), which means that the maximum error is 0.125 chip. In high sensitivity situations, the wrong position maybe have a higher peak than the correct position sometimes, so the maximum code phase error of L1 is considered 0.25 chip here.

Therefore, when transferring from L1 acquisition to L5 acquisition, the total code phase search space is from  $(C_{L5} - 6.5)$  to  $(C_{L5} + 6.5)$ .

#### VI. II Architecture and resource analysis

The architecture of the improved L5 acquisition aided with L1 is shown in Fig. 4. Since the code search space is reduced a lot, the use of FFT is no more needed and a bank of correlators can be used instead to search the 27 code phases in parallel (as half chip spacing is used for the code search).

The resource analysis is shown in Table 8.

So the whole resources needed are ALMs: 3.95 %, DSP: 0 %, RAM: 0.39 %.

From the estimation of the resources above, it can be seen that the resources needed are significantly reduced.

#### VI.III Acquisition time analysis

Since there is only one frequency to test, the time needed is as follows:

$$T_{all} = 1.58 + \frac{20.48 \times 10^6 \times 1.58}{204.8 \times 10^6} = 1.738 \text{ s} \quad (19).$$

So it can be seen that using the information obtained from the acquisition of the L1 signal, the frequency search space and thus the acquisition time are tremendously decreased. The 99 % acquisition time for L5 signal can be saved.

Module	ALMs	DSP	FPGA RAM (bit)
Carrier generator NCO and mixer	88		
Code generator Coherent accumulator in 1 ms	39.1	27.5	10 230
RAM (coherent) Coherent accumulator in 40 ms			1080
Magnitude calculator	90		
Non coherent accumulator	43.3		700

Table 8 Resource needed for L5 signal acquisition aided by L1 acquisition

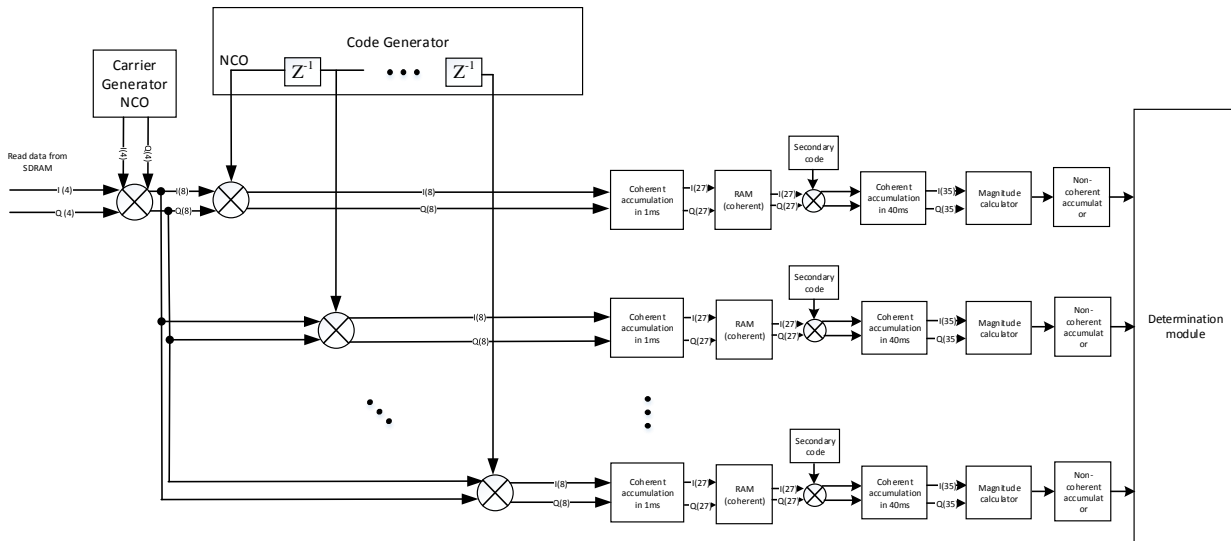


Fig. 4 Architecture of L5 acquisition aided by L1.

### VII CONCLUSION

As it is known that space applications always require small volume and small mass components, a reduced computational burden can be precious.

The algorithm and architecture above use the Doppler frequency and the code phase obtained during the acquisition of an L1C/A signal to help the L5 acquisition. As a result, the search space can be significantly reduced, which implies an important reduction of the resources and of the acquisition time.

It can be seen that 7 % ALM, 18 % DSP and 47 % RAM (ALTERA EP3SE260F) can be saved, and 99 % of the L5 acquisition time can also be saved compared with a traditional L5-only acquisition method and architecture.

### REFERENCES

- [1] James J. Miller, "Enabling a Fully Interoperable GNSS Space Service Volume", 6<sup>th</sup> International Committee on GNSS (ICG), Tokyo, Japan, September 5-9, 2011.
- [2] Elliott D. Kaplan, Christopher J. Hegarty, "Understanding GPS", Artech house, 2005.
- [3] V. Capuano, C. Botteron, Y. Wang, J. Tian, J. Leclère, P. -A. Farine, "GNSS/INS/Star Tracker Integrated Navigation System for Earth-Moon Transfer Orbit", in proc. of the ION GNSS+, September 2014.
- [4] C. Wang, R. A. Walker, M. P. Moody, "An Improved Single Antenna Attitude System Based on GPS Signal Strength", in proc. of the AIAA Guidance, Navigation, and Control Conference and Exhibit, 15-18 August 2005.
- [5] F. van Diggelen, "A-GPS: Assisted GPS, GNSS and SBAS", Artech house, 2009.
- [6] <http://www.spirentfederal.com/gps/Products/GSS8000/Overview/>, last accessed on 9<sup>th</sup> September 2014.
- [7] V. Capuano, C. Botteron, P. -A. Farine, "GNSS Performance for MEO, GEO and HEO", in proc. of the 64<sup>th</sup> International Astronautical Congress, October 2013.
- [8] F. Förster, Manual of the Fraunhofer Triband Front End L1/L2/L5 USB, December 2011.
- [9] <http://www.terasic.com.tw/cgi-bin/page/archive.pl?Language=English&CategoryNo=39&No=260>, last accessed on 9<sup>th</sup> September 2014.
- [10] M. L. Psiaki, "Block Acquisition of Weak GPS Signals in a Software Receiver", in proc. of the ION GPS, September. 2001.
- [11] J. Leclère, C. Botteron, P. -A. Farine, "Comparison Framework of FPGA-Based GNSS Signals Acquisition Architectures", IEEE Transactions on Aerospace and Electronic Systems, vol. 49, no, pp. 1497–1518, July 2013.

- [12] N.I. Ziedan, J. L. Garrison, "Unaided Acquisition of Weak GPS Signals Using Circular Correlation or Double-Block Zero Padding", in proc. of the of the IEEE Position Location and Navigation Symposium (PLANS), 2004.
- [13] L. Deambrogio, F. Bastia, C. Palestini, R. Pedone, M. Villanti, G. Corazza, "Cross-band Aided Code Acquisition in Dual-Band GNSS Receivers", IEEE Transactions on Aerospace and Electronic Systems, vol. 49, no. 4, pp. 2533–2545, October 2013.
- [14] R.N. Thessin, "Atmospheric Signal Delay Affecting GPS Measurements Made by Space Vehicles During Launch, Orbit and Reentry", MSc thesis, Massachusetts Institute of Technology, June 2005
- [15] [http://www.navipedia.net/index.php/Ionospheric\\_Delay](http://www.navipedia.net/index.php/Ionospheric_Delay), last accessed on 9<sup>th</sup> September 2014.
- [16] P. F. Silva, H. D. Lopes, T. R. Peres, J. S. Silva, J. Ospina, F. Cichocki, F. DAVIS, L. Musumeci, D. Serant, T. Calmettes, I. Pessina, J. V. Perelló, "Weak GNSS Signal Navigation to the Moon", ION GNSS+, 2013.